Phase Behavior and Polymerization Kinetics of a Semifluorinated Lyotropic Liquid Crystal

Christopher L. Lester and C. Allan Guymon*

Department of Polymer Science, University of Southern Mississippi, Hattiesburg, Mississippi 39406-0076

Received February 3, 2000; Revised Manuscript Received May 22, 2000

ABSTRACT: Recently, amphiphilic monomers that are capable of forming lyotropic liquid crystalline phases have been utilized in a variety of applications including emulsion polymerization, development of nanocomposites, and the formation of polymeric surfactants. A new class of fluorinated amphiphilic monomers that exhibit lyotropic mesophases has shown great promise in ophthalmic applications. Initial studies indicate that the monomer possesses a lamellar morphology at certain concentrations that when polymerized would yield a material with anisotropic properties ideal for repairing retinal tears. Characterization of the polymerization kinetics of these fluorinated monomers provides a better understanding of conditions such that structure retention can be obtained. The fluorinated amphiphiles exhibit varying phase morphology ranging from an isotropic micellar phase to discontinuous cubic and lamellar liquid crystalline phases with increasing concentration and variation in the percent neutralization of the acid moiety. The lyotropic liquid crystalline order changes significantly with respect to percent neutralization. The polymerization kinetics follow a trend of decreasing order with increasing neutralization in that the fastest rates are seen in samples with higher degrees of order specifically in the lamellar liquid crystalline phase. The polymerization rate decreases to a minimum in samples of cubic morphology with low degrees of overall order. The higher polymerization rates in the lamellar phase are due to a decrease in the termination rate. Additionally, the polymerization behavior and morphology have a tremendous impact on the resulting polymer.

Introduction

The organized nature of polymerizable amphiphiles in aqueous solution yields opportunities for novel biomedical applications, applications in membrane mediated chemistries, synthesis of novel nanocomposite materials, and in separation technology. These amphiphilic monomers, when dispersed in water at high enough concentration, form a variety of ordered structures. The type and amount of order in a given system are dependent on the concentration of amphiphile, temperature, pH, and ionic strength. The simplest order possible in a binary system at low amphiphile concentration is that of a spherical micelle. At higher concentrations in water, amphiphilic monomers may also form lyotropic liquid crystalline (LLC) phases including extended cylindrical micelles packed in a hexagonal array and lamellar aggregates with polar exteriors and water between the lamellae. Other lyotropic mesophases include cubic arrays of spherical micelles or inverse micelles.[1−3]

The use of perfluoroalkyl moieties in amphiphilic monomers and LLC systems has increased dramatically of late because of their unique properties including low surface energy and biocompatibility. These materials produce novel amphiphilic type structures with phase behaviors much different than classical hydrocarbon surfactants. Recently, novel surface active perfluoroalkyl monomers for use in ophthalmic compositions and other such applications have been developed in which a self-assembling biocompatible polymer precursor could be injected and polymerized. Current technology utilized in ophthalmic repair relies heavily on materials that are nonadhesive and possess little structural integrity. Consequently, retinal tears repaired with conventional techniques often fail. Some adhesive materials have been used in retinal repair that yield rigid attachments of the retina to the surrounding tissue which does not yield enough flexibility for the kind of stresses applied to the tear, often causing failure of the repair as well. Fluorinated LLC materials may be ideal for retinal repair in that they can act as a bioadhesive and have flexibility imparted by the anisotropic properties of the polymerized mesophase.[4] Little has been done, however, to characterize the lyotropic mesophases formed by these materials and the role that the structure plays in the polymerization mechanism and polymer structure.

The LLC phases formed by amphiphilic monomers, including those with fluorinated moieties, present a tremendous opportunity to study the impact of local ordering on the polymerization kinetics. One area of considerable interest is the retention of lyotropic structure after polymerization in aqueous mesophases so that these materials can be used in applications that require a well-defined nanostructure. A considerable amount of difficulty exists in retaining the original phase structure of these types of materials. In a series of papers, McGrath et al. studied a variety of polymerizable surfactants consisting of different monomer types, polar headgroups, and placement of the polymerizable group.[5−8] Retention of the liquid crystalline structure was not always successful, and if some lyotropic structure was retained, it was attributed to the formation of oligomers and not high molecular weight polymers. In other cases lyotropic structure has been retained, but it is not necessarily of the same phase structure of the monomers. For example, anionic polymerizable lyotropic liquid crystals in a hexagonal phase have been shown to convert to a lamellar phase upon polymerization.[9]

* To whom correspondence should be addressed.

10.1021/ma000197f CCC: $19.00
Published on Web 07/08/2000

While many studies have shown that development of lyotropic structure in polymers formed from amphiphillic monomers is possible, the structure is highly dependent on the type of monomer and on the polymerization conditions. Gin and co-workers have shown retention of inverse hexagonal phases of a variety of monomers. The structure retention was attained with a high degree of cross-linking. These highly ordered materials may be used in a variety of applications including catalysis, encapsulation, and nanocomposite synthesis.[10−12] Other cases of retained lyotropic order have also been reported but with limited information on the polymerization process yielding the desired morphologies.[13−24] A better understanding of the polymerization mechanism itself could help elucidate the optimal conditions for polymerizing lyotropic liquid crystalline monomers to unlock their tremendous potential for a variety of applications.

Lyotropic mesophases of polymerizable lipids have also been characterized with additional information about the effects of the LLC structure on the polymerization kinetics. The instantaneous polymerization rate and conversion of a variety of monomers have been studied. The polymerization rate, percent conversion, and the molecular weight were influenced greatly by ordered assemblies assumed by these structures.[25,26] Changes in activation energy and collision frequency were cited as reasons for the observed difference in polymerization kinetics.[27] However, many of the studies performed to date with polymerizable lyotropic liquid crystals have dealt with characterization before and after polymerization with little examination of the polymerization itself. Also, real-time analysis of the polymerization kinetics of such systems has not been carefully studied to further elucidate the impact such ordered assemblies have on the overall polymerization behavior.

The polymerization of a variety of conventional monomers solvated in lyotropic liquid crystals has also been attempted in order to template the unique nanostructure of these systems.[28−32] Templating the lyotropic liquid crystalline order onto a polymer system has proven difficult and in many cases has yielded nanostructures that result from phase separation and not from the liquid crystalline arrays.[28,29,33] To date, the impact of these ordered arrays on the polymerization kinetics has not been established.

On the other hand, the role of order in thermotropic liquid crystalline systems has been the focus of a number of studies. Interestingly, the polymerization of liquid crystalline monomers may be dramatically faster in smectic liquid crystalline phases than in the isotropic phase. This accelerated rate behavior has been attributed to a significant decrease in termination in the ordered phase.[34,35] Other studies have focused on the polymerization of small amounts of both aliphatic and liquid crystalline monomers dispersed in low molar mass thermotropic liquid crystals. In fact, a number of monomers with different properties and chemical structure have been shown to exhibit dramatic increases in polymerization rate as the order of the phase increased, even with decreasing temperatures. This behavior is induced by monomer segregation, which decreases the termination rate constant in some instances and increases the propagation and termination rate constant in others.[36−39] These studies have helped elucidate the role of order and structural evolution of polymerizations

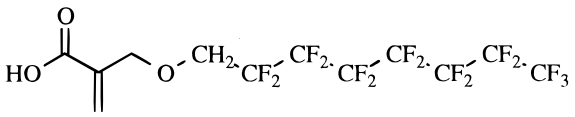

Figure 1. Chemical structure of the ether-substituted perfluoroalkyl methacrylic acid designated C8F7.

in organized media. Similar information about the polymerization in lyotropic systems could give a wealth of information on both the formation of lyotropic liquid crystalline order in polymers and how to optimize this structure for selected applications.

The polymerization kinetics and consequently the ultimate order of the polymer formed by fluorinated amphiphiles may therefore depend significantly on the different types of ordered phases assumed by these monomers. Conversely, the overall structure of the resulting material may be affected by the polymerization mechanism. The goal of this work is to examine the polymerization kinetics of a fluorinated amphiphile and correlate these kinetics to the phase behavior under a variety of conditions to form the basis for developing favorable morphologies for opthalmic repair. To determine the effect of different types of lyotropic ordering on the polymerization behavior and the ultimate polymer morphology, the phase behavior must first be determined. Phase behavior will be characterized in these lyotropic systems with changing temperature, concentration, and pH. Upon successful characterization of the phase behavior, the polymerization behavior of the fluorinated amphiphile in water will be also examined under conditions that change both the amount and type of LLC ordering. A systematic study examining the polymerization kinetics of these fluorinated polymerizable LLCs will elucidate details about the effect of ordering on the polymerization mechanism and help to optimize conditions for retention of structure. As the polymerization mechanism in different lyotropic mesophases is further better understood, correlation to polymer morphology and structure retention will be studied. An understanding of the effects of the order on polymerization will greatly facilitate the development of surface-active monomers not only for opthalmic applications but also for new polymeric materials such as tissue scaffolding, delivery systems for oil-soluble materials, and media for membrane-mediated chemistries with controlled structure and morphology.

Experimental Section

Materials. The surface-active monomer used in this study is an ether-substituted perfluoroalkyl methacrylic acid (C8F7).[4] The chemical structure of the monomer is shown in Figure 1. Deionized water and NaOH were used in formulating the lyotropic liquid crystal compositions. The photopolymerizations were initiated using Irgacure 2959 (Ciba-Geigy, Tarrytown, NY). The C8F7/water solutions were prepared with initiator concentrations approximately 5 wt % of the total monomer concentration.

Procedure. Small-angle X-ray scattering (Siemens XPD 700P WAXD/SAXS) with a Cu Kα line of 1.54 Å was used both to characterize the phase behavior of the systems and to determine the relative degree of ordering in the various samples. Bragg's law was used to determine the *d* spacing of the lyotropic mesophase. The ratio of peak height to width at half-height was utilized to determine the relative degree of order. A polarized light microscope (Nikon Optiphot-2 pol) equipped with a hot stage (Instec, Boulder, CO) was utilized

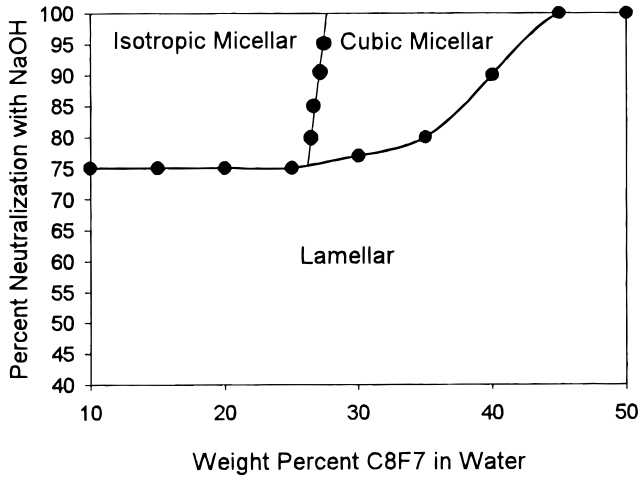

Figure 2. Phase diagram of C8F7/water with different mole percent neutralizations.

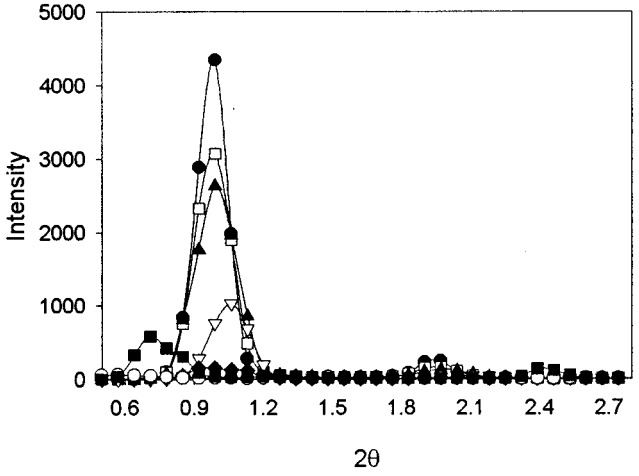

Figure 3. SAXS profiles of 40 wt % C8F7 in water as a function of mole percent neutralization. Shown are neutralizations of 40% lamellar (●), 50% lamellar (□), 60% lamellar (▲), 70% lamellar (▽), 80% lamellar (◆), 90% cubic (○), and 100% cubic (■).

to corroborate data collected with SAXS by looking for characteristic textures of the various mesophases.

Reaction profiles were monitored in real time with a differential scanning calorimeter (Perkin-Elmer DSC-7) modified with a medium-pressure UV arc lamp. Samples of approximately 10 mg were used and covered with a thin film of FEP (Du Pont fluorinated copolymer) in order to prevent evaporation of water. The DSC cell was purged with nitrogen for 10 min prior to exposing the sample to the UV light source in order to prevent oxygen inhibition during the polymerization. The samples were also heated to 80 °C and cooled to 30 °C at 10 °C/min in order to ensure uniform thickness and good thermal contact. Polymerizations were initiated with both full beam light and monochromatic 365 nm light with intensities of 34 and 3.75 mW/cm^2, respectively. The DSC sample cell was also attached to a refrigerated circulating chiller to ensure isothermal conditions.

The heat of polymerization was utilized to directly calculate the rate of reaction and the maximum rates of polymerization.[36] For these studies the theoretical value of 13.5 kcal/mol was used as the heat evolved per double bond reacted.[40] To determine individual rate parameters of termination and propagation, a series of after-effect experiments were performed. First the lumped kinetic constant $k_p/k_t^{1/2}$ was measured as a function of time from the polymerization rate profile. Then, by turning off the UV light source at various times during the polymerization process, the initiation step is eliminated, thus making it possible to decouple the propagation and termination rate parameters. This method of determining individual rate parameters is described in detail elsewhere.[36]

Results and Discussion

To determine the impact that the highly ordered nanostructure of this unique LLC has on polymerization kinetics, careful characterization of the phase behavior of the monomer was performed. As determined by polarized light microscopy, the C8F7 monomer forms lyotropic aggregates over wide ranges of composition and temperature. The lyotropic mesophases of the C8F7 monomer can be seen in Figure 2 which shows the phase diagram as a function of C8F7 concentration and percent neutralization. By changing the percent neutralization, the degree and type of lyotropic ordering is altered, even with samples at the same temperature and water/LLC composition. As can be seen in Figure 2, the desired lamellar mesophase exists over wide ranges of composition and temperature. The lamellar mesophase is observed at neutralizations below 70% and at concentrations as low as 10 wt % C8F7. At neutralizations of 75% or higher, an isotropic micellar phase appears at concentrations ranging from approximately 25% down to well below 5% C8F7. This behavior is due to the fact that both lower concentration and higher percent neutralizations induce curvature at the interface because of increased ion−ion repulsion. At concentrations of 25% to 40% C8F7 at neutralizations higher than 75%, the concentration of micelles is such that they become close packed into a cubic liquid crystalline phase. At concentrations greater than 45% C8F7, the lamellar phase is seen at all neutralizations.

Similar phase behavior is observed with increasing concentration of C8F7 if the monomer is in its fully ionized state, which corresponds to 100% neutralization. Below 25 wt % C8F7, the mesophases appear to be isotropic micellar as no well-defined peaks are observed in small-angle X-ray scattering experiments. Above 25%, C8F7 X-ray diffraction patterns and polarized light microscopy indicate a discontinuous cubic array of regular micelles. After increasing to 45 wt % C8F7, the lamellar mesophase is attained. The C8F7/water mixtures remain lamellar with increasing compositions of C8F7 up to at least 70 wt %.

As previously stated, the goal of this work is to determine the effect these different ordered structures has on the polymerization kinetics. To achieve this goal, it was important to choose a formulation of C8F7 that exhibits various different liquid crystalline phases. For this reason samples of 40% C8F7 with neutralizations ranging from 40% to 100% were chosen as the focus of study. At this concentration, neutralizations of 40−80% all exhibit lamellar liquid crystalline characteristics. The samples with neutralizations of 90% and 100% exhibit no lamellar textures and are optically isotropic. This particular phase is a discontinuous cubic phase of normal micelles due to its optically isotropic nature and the liquid crystalline order observed with the SAXS experiments. The bicontinuous cubic phase can be ruled out because the viscosity of the samples is lower than that of the lamellar phases whereas the opposite is true if a bicontinuous cubic phase is present.[1]

SAXS was not only used to determine phase behavior of these materials but also to yield qualitatively the relative degree of order observed in samples with varying percent neutralizations. In Figure 3 SAXS profiles of the 40% C8F7/water system with varying

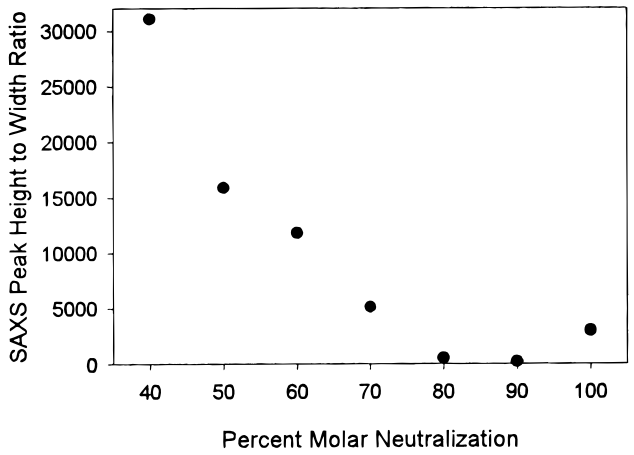

Figure 4. Ratios of peak height to width at half-height of 40 wt % C8F7 as a function of percent neutralization.

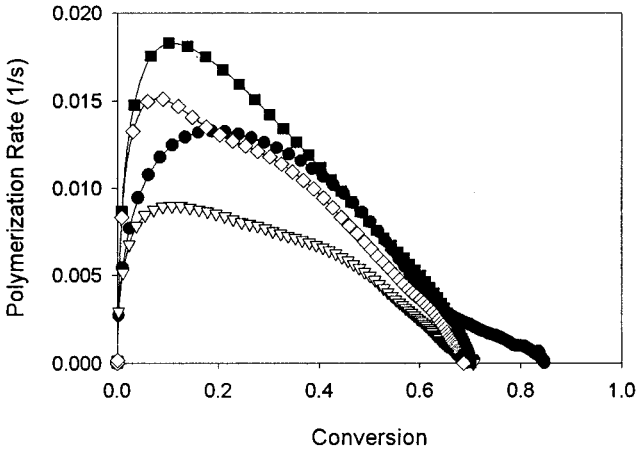

Figure 5. Polymerization rate versus extent of double bond conversion of 40 wt % C8F7 in water with varying mole percent neutralizations. Shown are neutralizations of 50% lamellar (◇), 60% lamellar (■), 90% cubic (▽), and 100% cubic (●).

mole percent neutralizations are shown, in which the relative scattering intensity has been plotted against the scattering angle. As can be seen, the relative degree of order decreases with increasing mole percent neutralization from 40% to 80% while remaining in the lamellar mesophase. It is important to note that the 40−80% neutralized samples all have a primary reflection at approximately the same scattering angle. Higher order peaks exist for these samples in the ratio of 1:2:3, which is characteristic of a lamellar mesophase. Upon increasing neutralization to 90%, the primary SAXS peak shifts to a lower angle, indicating a phase change to the cubic liquid crystalline phase. Also, the ratio of the scattering angles of the peaks observed in this sample does not correspond to hexagonal or lamellar patterns. Interestingly, the diffraction peak observed in the 90% sample is much smaller than the other peaks at different neutralizations. When the mole percent neutralization is increased to 100%, the peak intensity again increases while remaining in the cubic liquid crystalline mesophase.

To determine more quantitatively the relative degree of order as a function of mole percent neutralization, for 40 wt % C8F7 in water, the peak heights obtained from SAXS were divided by the peak width at half-height as seen in Figure 4. The ratio of peak height to width yields a value that, when compared to similar samples, should be indicative of the relative degree of order in a sample and should compensate for differences in position and thickness. The peak height to width at half-height ratio is a good measure of relative degrees of LLC ordering by corroborating evidence from order parameters obtained from the quadrupolar splitting of ^{2}H NMR.[41] The 40% neutralization exhibits the highest degree of order with a sharp decrease when increasing neutralization to 50%. At both of these neutralizations, some crystalline material is still observed using the polarizing microscope. A significant monotonic decrease in the peak height-to-width ratio occurs from 50% through 80%. The cubic liquid crystalline phase neutralized 90% exhibits the least amount of order. By increasing the neutralization to 100%, higher degrees of order are again induced. This phenomenon is due to increasing charge−charge repulsion, which increases the amount of curvature of the interface with increased ionization up to 90% and then at higher neutralization ion shielding allows an increase in order within the cubic liquid crystalline phase.

Not only does the type and degree of order change with different compositions, but distinct differences in the polymerization behavior are also observed as the amount and type of order of the LLC monomer change. Figure 5 shows the polymerization rate for a 40 wt % C8F7 system as a function of conversion for various mole percent neutralizations. The highly ordered lamellar sample neutralized 50% polymerizes readily but is not observed to polymerize as quickly as the 60% neutralized sample of lesser overall order. This behavior is due to the existence of the coexisting crystalline phase at lower neutralizations. Even though the crystalline domains are highly ordered, they lack sufficient mobility to enhance polymerization rate. The 60% neutralized sample, a homogeneous lamellar liquid crystalline phase with a relatively high amount of liquid crystalline order, exhibits the fastest rate profile. As the percent neutralization increases, the rate decreases until a minimum rate is observed at 90% neutralization. Upon increasing the neutralization to 100%, which increases the observed order, the rate increases again. Interestingly, the polymerization behavior for the full range of neutralizations follows the relative degree of order of these samples very closely. With increasing neutralization, lower degrees of ordering are observed, and consequently the polymerization rate decreases. Then, when the order again increases in the cubic phase, the rate increases as well.

This trend becomes even more apparent when the maximum polymerization rate for polymerizations of 40 wt % C8F7 in water is plotted as a function of mole percent neutralization as seen in Figure 6. The 40% neutralized sample exhibits a peak rate lower than the 50% neutralized sample, and upon neutralization to 60% the highest peak rate was observed. The 40% and 50% neutralized samples had lower peak rates than the 60% neutralization despite more observed order, but this was attributed to the fact that the 40% and 50% neutralized samples were not homogeneous lamellar phases at the temperature of the polymerization. As stated previously, crystalline domains exist at at these particular neutralizations. From the maximum polymerization rate observed at 60% neutralization, a steady decrease in peak polymerization rate is observed with increasing neutralization up to 80% within the lamellar mesophase. Although these materials are still in a lamellar phase, the decrease may be attributed to slight increases in

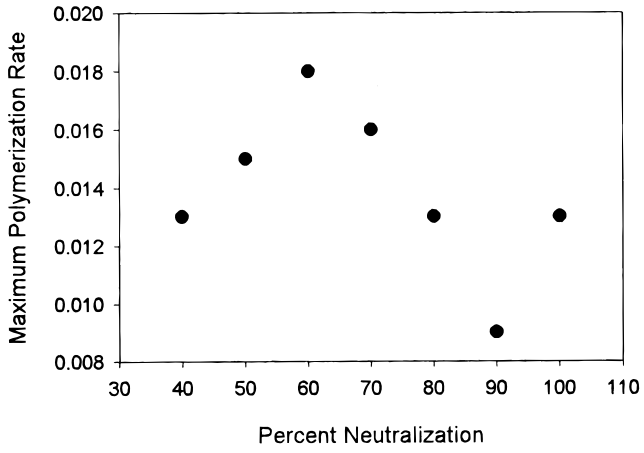

Figure 6. Maximum polymerization rate of 40 wt % C8F7 in water as a function of percent neutralization.

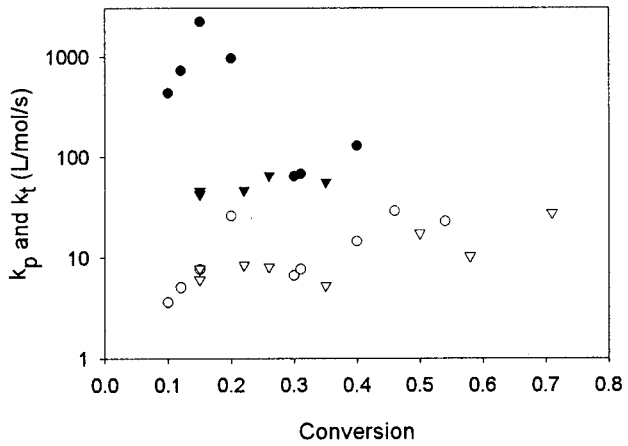

Figure 7. Termination (k_t) and propagation (k_p) rate parameters of 40% C8F7/water shown as a function of double bond conversion. Given are neutralizations of k_t 90% cubic (●), k_t 60% lamellar (▼), k_p 90% cubic (○), and k_p 60% lamellar (▽).

curvature of the interface resulting from the increasing ion−ion repulsion. The lowest polymerization rate is observed when the neutralization is increased to 90%, which induces the lowest amount of order within the cubic liquid crystalline phase. Upon increasing the neutralization to 100% and consequently to higher degrees of ordering in the cubic liquid crystalline phase, a higher peak rate was observed.

To determine the driving force behind these changes in polymerization behavior, individual rate parameters for propagation and termination were determined. Figure 7 shows the propagation and termination rate parameters for both the lamellar and the cubic phase containing 40 wt % C8F7, neutralized 60% and 90%, respectively. These two neutralizations correspond to the highest and lowest observed polymerization rate. As seen in the figure, the propagation rate parameters for both samples are essentially the same within experimental error over the range of conversions measured, implying that the force driving these changes must be termination, not propagation. This is in fact the case after close examination of the termination parameter. At low conversions over the range in which maximum polymerization rates are observed, the termination rate parameter for the lamellar liquid crystalline sample which has the highest polymerization rate is shown to be an order of magnitude less than that of the cubic mesophase. The lower values of k_t correspond

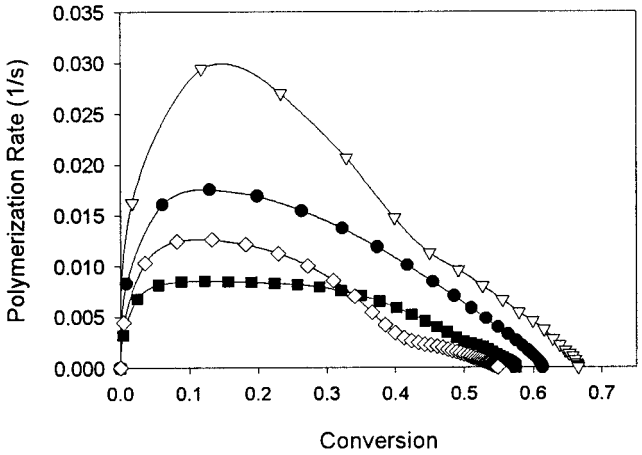

Figure 8. Polymerization rate versus extent of double bond conversion of 30 wt % C8F7 in water with varying mole percent neutralizations. Shown are neutralizations of 50% lamellar (●), 70% lamellar (▽), 90% cubic (◇), and 100% cubic (■).

to slower termination rates, which yields more propagating radicals and consequently increases the overall polymerization rate. At higher conversions, the k_t of the 90% neutralized sample actually became depressed to levels approximately equal to those in the 60% neutralized sample. This behavior can be attributed to a change in phase during polymerization, which causes an acceleration of the polymerization rate, and is observable, by distinct changes in the rate profiles at the same conversions.

This type of kinetic phenomenon is not unique to the 40 wt % C8F7 composition. Similar trends are also observed in the 30 wt % C8F7 system. In Figure 8, the rate profiles of the 30 wt % C8F7 sample with varying mole percent neutralization are plotted as a function of extent of double bond conversion. With increasing percent neutralization up to 70% in the lamellar mesophase, the fastest polymerization rate profile is observed. Interestingly, the 50% neutralized sample exhibits a lower rate than the 70% sample despite a higher degree of lamellar order. It is possible that the 50% neutralized sample possesses such a high degree of order that even though it is liquid crystalline, the mobility is not great enough to allow enhancement of the polymerization rate. The polymerization rates decrease with increasing neutralization to a minimum at 90%, which corresponds to the cubic liquid crystalline phase. Interestingly after increasing the neutralization further to 100%, increased rates are once again observed as in the 40% C8F7/water system with the increase in order.

Other studies have shown that the percent ionization or neutralization can have a significant impact on the polymerization kinetics of ion-containing monomers.[42] Obviously, as the neutralization is varied in the C8F7 systems, the ionic strength also changes. To determine whether ionic strength also influences the polymerization behavior and that the observed changes are due to ordering effects, C8F7 samples neutralized to the same extent with varying ionic strength were formulated and studied. The ionic strength was varied by the incremental addition of NaCl. Figure 9 shows polymerization rate profiles of a sample containing 30% C8F7 with 50% neutralization but varying ionic strength. All of the samples exhibit a lamellar morphology with increasing salt concentration. The sample with no added salt exhibits the fastest polymerization rate, and small

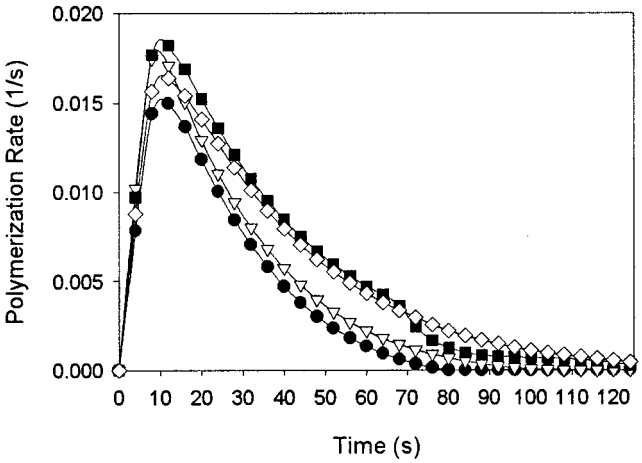

Figure 9. Polymerization rate as a function of time of 30 wt % C8F7 in water at constant neutralization of 50% with varying ionic strength. Shown are percent NaCl 10% lamellar (●), 20% lamellar (▽), 30% lamellar (◇), and 40% lamellar (■).

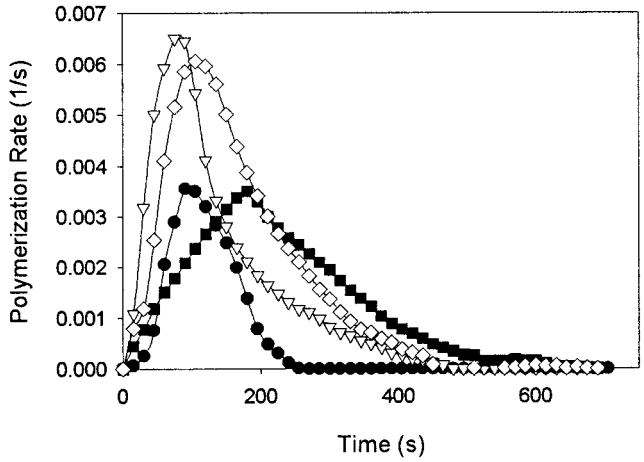

Figure 10. Polymerization rate versus time of C8F7/water samples neutralized 100% at varying concentrations. Shown are concentrations of 20% isotropic (●), 30% cubic (▽), 40% cubic (■), and 45% lamellar (◇).

changes are observed with subsequent additions of salt. The greatest difference observed is between the sample without NaCl and the one with 40% NaCl, but even in this extreme case the difference is slight. It can clearly be seen that the polymerization behavior is impacted more greatly by the degree and type of order in the system rather than the ionic strength.

As it is also possible to vary the phase behavior of this system by varying the concentration as well as the mole percent ionization, kinetic experiments were performed at constant neutralization and with varying C8F7 concentration. Polymerization rate profiles can be seen in Figure 10 of samples neutralized 100% with concentrations varied such that the full variety of phases in the C8F7 system are observed. The polymerization rate profile of the isotropic micellar phase at 20 wt % C8F7 is observed to be slower than the ordered cubic phase of 30% C8F7 by a factor of 2. Upon increasing the concentration further to 40 wt % C8F7, a 2-fold drop in polymerization rate occurred as a result of being in a less ordered cubic liquid crystalline phase. Upon increasing concentration well into the lamellar phase, the polymerization rate increased back to the peak rate observed in the cubic phase at 30%. As previously stated, changes in concentration and neutralization both cause changes in lyotropic liquid crystalline morphology. The kinetic results for both means of modulating phase characteristics yield similar polymerization behaviors in that the more highly ordered liquid crystalline phases exhibit faster polymerization rates.

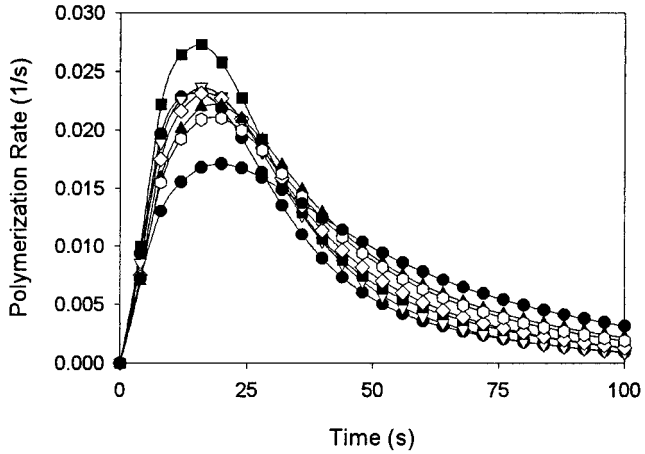

Figure 11. Polymerization rate versus time of varying concentrations of C8F7/EGDAc solutions. Shown are concentrations of 20% (●), 25% (▽), 30% (■), 35% (◇), 40% (▲), 45% (○), and 50% (◆).

To verify whether this phenomenon could be attributed to mere concentration effects or is due to the unique morphologies of the various phases, polymerization rate profiles were obtained of C8F7 in ethylene glycol diacetate (EGDAc). C8F7/EGDAc solutions of varying concentration were shown to have no observable lyotropic mesophases, and upon polymerization a relatively linear dependence on monomer concentration was observed as can be seen in Figure 11. Slight increases in peak polymerization rates can clearly be seen when increasing concentration from 20% to 35%. Upon increasing to 40 wt % C8F7 a larger increase in rate is observed, but this could be attributed to increasing viscosity of the solution. After increasing the concentration further to 45% and 50%, the rate drops slightly, which could be due to diffusional limitations of this particular system. The important point to note is that the polymerization of C8F7 in EGDA exhibits a more typical dependence on monomer concentration than the polymerization in its ordered phases in water, which implies that the changes in rate are due to ordering effects and not concentration.

As varied kinetic behavior is observed in the C8F7/water system with varying phase behavior, some initial studies were performed to determine whether these differing polymerization behaviors have any impact on the retention of the original nanostructure of the material. In Figure 12 the peak height to width at half-height of the primary SAXS peaks are shown for the 60% and 90% neutralized samples of the 40 wt % C8F7/water system at varying amounts of cure time. Once again, these samples correspond to the lamellar and cubic mesophases, respectively, where the lamellar phase exhibits the fastest polymerization rate with a high degree of LLC order and the cubic phase shows depressed polymerization rates and the lowest degree LLC order. For the lamellar LLC sample that exhibits the fastest polymerization rate, the original nanostructure is retained even at long cure times. At extended cure times, some loss of order is apparent, but this could be

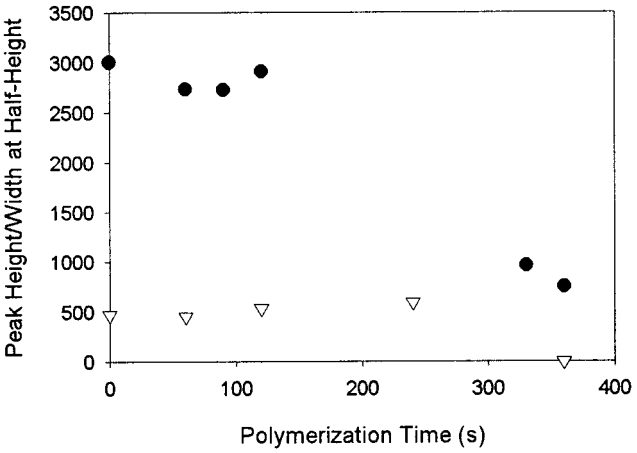

Figure 12. Ratio of peak height to width at half-height for various cure times of 40 wt % C8F7 in water at neutralizations of 60% lamellar (●) and 90% cubic (▽).

attributed to the inevitable volume contraction experienced upon vinyl polymerization. This type of structure retention is not observed in the 90% neutralized sample that has the slowest polymerization rate. Here, a complete disruption of the original liquid crystalline order at higher cure times is observed. From these preliminary results, it is apparent that the polymerization behavior has a large impact on structure retention. This influence of polymerization kinetics on structure retention will be more fully explored in future work.

Conclusions

This work presents the photopolymerization behavior and kinetics of a semifluorinated amphiphile in its various LLC phases. The phase behavior of this LLC monomer is characterized with respect to pH and concentration and is shown to have two primary liquid crystalline phases: the lamellar and cubic as well as an isotropic micellar phase. The degree and type of liquid crystalline order decrease to a minimum with increasing ion−ion repulsion as mole percent neutralization is increased or as the concentration of monomer is decreased. The photopolymerization rate is significantly faster in samples with increased extents of order. Rate acceleration is observed when the phase morphology is altered by changing the monomer concentration. Again, the degree of order corresponds to faster rates. The rate acceleration for these systems is driven by a decrease in the termination rate. Ionic strength does not appear to be a significant contributing factor in the changes in polymerization behavior. The effects of increasing concentration were also evaluated in a nonaggregating solvent as a control experiment. These results indicate that differences in polymerization behavior are solely due to the unique morphologies of the LLC systems. Initial studies indicate that the liquid crystalline systems with enhanced rates retain the original nanostructure to a larger extent than the liquid crystalline systems with slower polymerization rates. In summary, the polymerization behavior of semifluorinated LLC monomers depends greatly on the phase morphology, with higher polymerization rates observed in more highly ordered systems, and the ultimate polymer structure appears to be impacted greatly by the polymerization kinetics.

Acknowledgment. The authors would like to thank the University of Southern Mississippi and Oak Ridge Associated Universities for financial support of this project. Dr. Lon J. Mathias is also gratefully acknowledged for providing the C8F7 monomer.

References and Notes

(1) Gray, G. W., Winsor, P. A., Eds.; *Liquid Crystals & Plastic Crystals*, 1st ed.; John Wiley & Sons: New York, 1974; Vol. 1.
(2) Kelker, H.; Hatz, R. *Handbook of Liquid Crystals*, 1st ed.; Verlag Chemie: Weinheim, 1980.
(3) *Polymerization in Organized Media*; Paleos, C. M., Ed.; Gordon and Breach Science Publishers: Philadelphia, 1992.
(4) Charles, S. T.; Hammer, M. E.; Lang, J. C.; Lochhead, R. Y.; Mathias, L. U.S. Patent 5,858,345, 1997.
(5) McGrath, K. M. *Colloid Polym. Sci.* **1996**, *274*, 399.
(6) McGrath, K. M.; Drummond, C. J. *Colloid Polym. Sci.* **1996**, *274*, 316.
(7) McGrath, K. M. *Colloid Polym. Sci.* **1996**, *274*, 499.
(8) McGrath, K. M.; Drummond, C. J. *Colloid Polym. Sci.* **1996**, *274*, 612.
(9) Thundathil, R.; Stoffer, J. O.; Friberg, S. E. *J. Polym. Sci., Polym. Chem.* **1980**, *18*, 2629.
(10) Gray, D. H.; Gin, D. L. *Chem. Mater.* **1998**, *10*, 1827.
(11) Deng, H.; Gin, D. L.; Smith, R. C. *J. Am. Chem. Soc.* **1998**, *120*, 3522.
(12) Smith, R. C.; Fischer, W. M.; Gin, D. L. *J. Am. Chem. Soc.* **1997**, *119*, 4092.
(13) Li, T. D.; Gan, L. M.; Chew, C. H.; Teo, W. K.; Gan, L. H. *Langmuir* **1996**, *12*, 5863.
(14) Lopez, E.; O'Brien, D. F.; Whitesides, T. H. *J. Am. Chem. Soc.* **1982**, *104*, 305.
(15) Koch, H.; Ringsdorf, H. *Makromol. Chem.* **1981**, *182*, 255.
(16) Kippenberger, D. J.; Rosenquist, K.; Odberg, L.; Tundo, P.; Fendler, J. H. *J. Am. Chem. Soc.* **1982**, *104*, 2000.
(17) Yuan, Y.; Tundo, P.; Fendler, J. H. *Macromolecules.* **1989**, *22*, 1947.
(18) Fendler, J. H.; Tundo, P. *Acc. Chem. Res.* **1984**, *17*, 3.
(19) Durairaj, B.; Blum, F. D. *Polym. Prepr.* **1985**, *26*, 239.
(20) Elias, H. G. *J. Macromol. Sci.* **1973**, *A7*, 601.
(21) O'Brien, D. F.; Whitesides, T. H.; Klingbiel, R. T. *J. Polym. Sci., Polym. Lett.* **1981**, *104*, 95.
(22) Tundo, P.; Kippenberger, D. J.; Klahn, P. L.; Prieto, N. E.; Jao, T. C.; Fendler, J. H. *J. Am. Chem. Soc.* **1982**, *104*, 456.
(23) Lee, Y. S.; Yang, J. Z.; Sisson, T. M.; Frankel, D. A.; Gleeson, J. T.; Aksay, E.; Keller, S. L.; Gruner, S. M.; O'Brien, D. F. *J. Am. Chem. Soc.* **1995**, *117*, 5573.
(24) Srisiri, W.; Sisson, T. M.; O'Brien, D. F.; McGrath, K. M.; Han, Y.; Gruner, S. M. *J. Am. Chem. Soc.* **1997**, *119*, 4866.
(25) Lei, J.; O'Brien, D. F. *Macromolecules* **1994**, *27*, 1381.
(26) Sells, T. D.; O'Brien, D. F. *Macromolecules* **1994**, *27*, 226.
(27) Lei, J.; Sisson, T. M.; Lamparski, H. G.; O'Brien, D. F. *Macromolecules* **1999**, *32*, 73.
(28) Antonietti, M.; Caruso, R. A.; Göltner, C. G.; Weissenberger, M. C. *Macromolecules* **1999**, *32*, 1383.
(29) Antonietti, M.; Hentze, H. P. *Colloid Polym. Sci.* **1996**, *274*, 696.
(30) Friberg, S. E.; Yu, B.; Ahmed, A. U.; Campbell, G. A. *Colloids Surf.* **1993**, *69*, 239.
(31) Candau, F.; Zekhnini, Z.; Durand, *J. Colloid Interface Sci.* **1986**, *114* 398.
(32) Holtzscherer, C.; Candau, F. *Colloids Surf.* **1988**, *29*, 411.
(33) Göltner, C. G.; Antonietti, M. *Adv. Mater.* **1997**, *9*, 431.
(34) Hoyle, C. E.; Watanabe, T. *Macromolecules* **1994**, *27*, 3790.
(35) Hoyle, C. E.; Mathias, L. J.; Jariwala, C.; Sheng, D. *Macromolecules* **1996**, *29*, 3182.
(36) Guymon, C. A.; Bowman, C. N. *Macromolecules* **1997**, *30*, 1594.
(37) Guymon, C. A.; Hoggan, N. A.; Rieker, T. P.; Walba, D. M.; Bowman, C. N. *Science* **1997**, *275*, 57.
(38) Guymon, C. A.; Bowman, C. N. *Macromolecules* **1997**, *30*, 5271.
(39) Guymon, C. A.; Dougan, L. A.; Martens, P. J.; Clark, N. A.; Walba, D. M.; Bowman, C. N. *Chem. Mater.* **1998**, *10*, 2378.
(40) *Encyclopedia of Polymer Science and Engineering*; Kroschwitz, J., Mark, H., Overberger, C., Bikales, N., Menges, G., Eds.; J. Wiley and Sons: New York, 1985; Vol. 1A.
(41) Dimitrova, G. T.; Tadros, T. F.; Luckham, P. F.; Kipps, M. R. *Langmuir* **1996**, *12*, 315.
(42) Anseth, K. S.; Scott, R. A.; Pepps, N. A. *Macromolecules* **1996**, *29*, 8308.

MA000197F